

INTERCOMPARISON OF GROUND-BASED AND SPACE
SOLAR FLUX MEASUREMENTS

Contract No. NASW-2568

SECOND
BI-MONTHLY TECHNICAL PROGRESS NARRATIVE

for Period

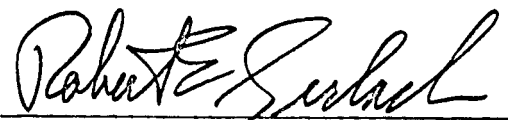
1 December 1973 through 31 January 1974

Prepared for
NASA Headquarters, Washington, D. C. 20546


Prepared By:

Aden B. Meinel
Dean B. McKenney
William T. Beauchamp

Reviewed By:


Robert E. Gerlach
Contract Administrator

Approved By:


Dean B. McKenney
Program Manager

HELIO ASSOCIATES, INC.
8230 East Broadway
Tucson, Arizona 85710

NASA-CR-137087) INTERCOMPARISON OF
GROUND-BASED AND SPACE SOLAR FLUX
MEASUREMENTS Second Bi-Monthly Technical
Progress Narrative, 1 Dec. 1973 - (Helio
Associates, Inc., Tucson, Ariz.) 39 p

N74-71705

Unclas
00/99 30843

TABLE OF CONTENTS

	List of Figures	ii
I.	Introduction	1
II.	Technical Progress Summary	2
III.	Current Problems	33
IV.	Work Planned for Next Period	34
	References	35

LIST OF FIGURES

Figure		Page
1	Description of Eppley Pyrheliometer	4
2	Sketch of the Moving Bar Occulting Radiometer (MBOR)	7
3	Photograph of the Moving Bar Occulting Radiometer (MOBR)	8
4	Typical clear-day output from the Moving Bar Occulting Radiometer (MBOR)	9
5	Detector cell design for the MBOR	11
6	Sketch of the Fixed Bar Occulting Radiometer (FBOR)	12
7	Photograph of the Fixed Bar Occulting Radiometer (FBOR)	13
8	Detector cell design FBOR	14
9	Photographs of instrument tower	16
10	Load line plot for a typical photodiode (UDT3DP)	20
11	Circuit schematic for the photodiode-operational amplifier circuit	20
12	Schematic diagram of Helio circuit used for the current-to-voltage transducer	21
13	Deviation from linearity of the silicon cell response for short-circuit operation	22
14	Recorder output 1/16/74 showing clear day comparison between (a) MBOR and (b) U/A records	26
15	Recorder output 1/19/74 showing partly cloudy day comparisons between (a) MBOP and (b) U/A records	27

Figure		Page
16	MBOR recorder output showing pattern typical for day with high thin clouds	29
17	MBOR recorder output showing pattern typical for an overcast day	30

1. INTRODUCTION

This is the second of three Bimonthly Progress Reports on the "Intercomparison of Ground-Based and Space Solar Flux Measurements", contract NASW-2568. Progress during the period from 1 December 1973 to 31 January 1974 is reported.

The objective of the 8-month contract is to establish instrumentation and data reduction procedures to be able to compare ground-based measurements with observations made from orbiting spacecraft. Short-term baseline data will be collected during the latter part of the contract.

Section II presents progress on those tasks underway during the period and Section III will discuss problem areas. Finally, the work planned for the next two-month period will be discussed in Section IV.

II. TECHNICAL PROGRESS SUMMARY

Task 2 Instrumentation

There are several instruments available today which have been designed specifically for solar insolation measurements. The line of instruments offered by Eppley Laboratories in Newport, R.I. is perhaps representative of the current state-of-the-art in commercial scientific instruments. The National Weather Service has used these instruments for many years to gather data over a network of approximately 80 stations in the United States. At the NOAA/NSF workshop on solar insolation held at Silver Spring, Md. in November 1973 there was a strong consensus of opinion that the data were both inadequate and inaccurate in most instances.

In this research, we are addressing the problem of the inadequacy of the data while maintaining reasonably high standards of accuracy. One of the main points of inadequacy discussed was a general lack of sufficiently detailed data for all weather conditions and locations. This research deals with the methodology and instrumentation needed to provide more adequate data for the user.

Several highly accurate absolute radiometers have been developed over the past several years. We have elected to use secondary radiometers which will allow greater ease of operation and better applicability of the data to current and future needs for solar insolation data. The instrument development task described here gives details of two instruments which are being

refined for this application.

The goal is to develop instruments to measure unambiguously two of the three following quantities: 1) the total solar flux on a horizontal plane, Φ_T ; 2) the direct (not scattered) flux either normal to the direction of the sun, Φ_{dn} , or on a horizontal plane, Φ_d ; 3) the diffuse (scattered) solar flux on a horizontal plane, Φ_D . In the literature¹ these quantities have also been called the global or G-radiation, the I-radiation, and the D-radiation respectively. To determine all three quantities, we must specify two of them since

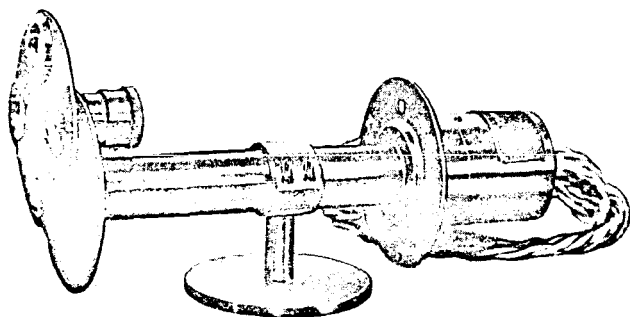
$$\Phi_T = \Phi_d + \Phi_D.$$

To accomplish this goal, two Helio Associates instruments were slightly modified to measure concurrently both the total and diffuse radiation fluxes. We have also included the use of an instrument to measure the direct normal radiation flux, Φ_{dn} , for comparison with data from the National Weather Service.

Task 2.1 Instrument Design

Task 2.2 Instrument Fabrication

The instrument to be used for measurement of Φ_{dn} is a standard Eppley pyrhelimeter (Model NIP), which is identical in physical design to the instrument in wide use by the National Weather Service for similar measurements. The Eppley description sheet for the pyrhelimeter is included in Figure 1. The optical arrangement of the instrument consists of a collimating tube and aperture with a 10 to 1 length to width ratio in front of a thermal



EPPLEY NORMAL INCIDENCE PYRHELIOMETER

For either total or spectral measurements of the
Direct Solar Intensity

The Eppley Normal Incidence Pyrheliometer, as its name implies, was designed for the measurement of solar radiation at normal incidence. In effect, it may be considered a thermoelectric version or variation of the Smithsonian Silver Disk Pyrheliometer, as it incorporates in its design some of the basic features of that instrument.

The sensitive element of the pyrheliometer is a E 6 type wire wound thermopile with a thermistor temperature compensating circuit if required, embedded in heat sink of thermopile. The receiver is coated with Parsons' black lacquer.

The resistance matches all standard type recording potentiometers very well but is not suitable for use with microammeter type recorders. The thermopile is mounted at the base of a brass tube, the aperture of which bears a ratio to its length of 1 to 10, subtending an angle of $5^{\circ} 43' 30''$. The inside of this tube is blackened and suitably diaphragmed; the outside is chromium plated. The tube is filled with dry air at atmospheric pressure and sealed at the viewing end by a removable insert carrying a crystal quartz window 1 mm. thick. Two flanges, one at each end of the pyrheliometer tube, are provided with a sighting arrangement for aiming the instrument directly at the sun. A manually rotatable disk which can accommodate three filters (such as Schott OG1, RG2 and RG8) and leave one aperture free for total spectrum measurements is provided.

The instrument is supplied on a circular base with screw holes for mounting. For periodic readings, the Pyrheliometer should be attached to a mount with provision for varying the elevation and the azimuth settings. If a continuous record is required, the pyrheliometer must be mounted on a power driven equatorial mount such as the Eppley Model EQM.

When the pyrheliometer has been mounted and the leads connected to the recorder or indicator, the tube should be aimed directly at the sun by positioning it so that the image of the sun through the small hole in the front flange of the tube falls directly on the "target" or small black spot on the inner side of the flange at the rear of the tube. Normal incidence readings may then be taken.

INSTRUMENT CHARACTERISTICS

Sensitivity	4-7 millivolts per $\text{cal cm}^{-2} \text{ min}^{-1}$
Impedance	approximately 200 ohms
Temperature dependence	± 1 percent over ambient temperature range -20 to $+40^{\circ}\text{C}$ (temperature compensation of sensitivity can be supplied over other ranges within the limits -70 to $+50^{\circ}\text{C}$ at additional charge).
Linearity	response linear up to intensities of $4 \text{ cal cm}^{-2} \text{ min}^{-1}$
Response time	1 second ($1/e$ signal)

Figure 1 Description of Eppley Pyrheliometer

pile detector. The angle of view for the detector through these optics is of the order of $\pm 5^\circ$ from normal. Therefore if the instrument is mounted on a polar mount so that it tracks the sun, it will detect the direct radiation flux, plus part of the circumsolar diffuse radiation. One of the six National Weather Service stations which perform measurements of direct normal solar flux is located at the Institute of Atmospheric Physics at the University of Arizona in Tucson. We, therefore, have ready access to official NWS data for comparison with the measurements by this instrument and the equipment of our own design.

Helio Associates' pyrhelimeter was sent to the Eppley Laboratories for overhaul and calibration on November 15, 1973. This work includes replacement of the thermal pile, cleaning, and calibration to their reference standards. Because of inclement weather, we are not yet in receipt of this instrument. We have taken the opportunity to use the mount, and a surplus pyrhelimeter housing, to run some tests on a commercially available Thermal Pile Detector made by Hewlett Packard Co. The use of this device has allowed us to check the tracking accuracy of the equatorial mount, and work out some design details and mounting requirements for the tracking instrument. Upon receipt of the pyrhelimeter, and a few days of direct comparison (side-by-side) with the university instrument, there will be minimal delay in making this equipment operational.

One of the instruments to be used for measurement of the total and diffuse fluxes is the Moving Bar Occulting Radiometer (MBOR).

A detailed sketch of this instrument is shown in Fig. 2, and a photograph of the instrument in its installed position is shown in Fig. 3. This instrument has a circular aperture over the detector. The 4.8mm diameter hole is located on the axis of revolution (North-South orientation) of a circular occulting bar. This bar is driven at a rate of 1/3 RPM, and has a cross section such that it casts a sharp shadow on the aperture once every three minutes. The width of the bar is specified by

$$w > d + 2R \sin(\frac{1}{2}^\circ) \quad (1)$$

where d is the aperture diameter and R is the radius of curvature of the bar. The bar may also be cut so that its arc length will be only as long as needed for the local maximum altitude of the sun, minimizing the correction factor for the diffuse component measurement. One of the correction factors which must be applied to the raw data takes account of the diffuse radiation which is lost to the detector due to the presence of the bar in the 2π steradian solid angle of view. When the bar is not in line with the sun the detector produces a signal proportional to the total flux or Φ_T . When the bar occults the sun, the detector signal is proportional to only the scattered light intensity or Φ_D . The resulting output vs. time is shown on the chart record in Fig. 4. The values of Φ_T , Φ_D , and Φ_d as obtained from these data are labeled for easy identification.

The overall size of this instrument is about 20 x 6.5 x 7 cm. It is therefore a compact package which is well suited to possible field operation. The detector is mounted beneath the

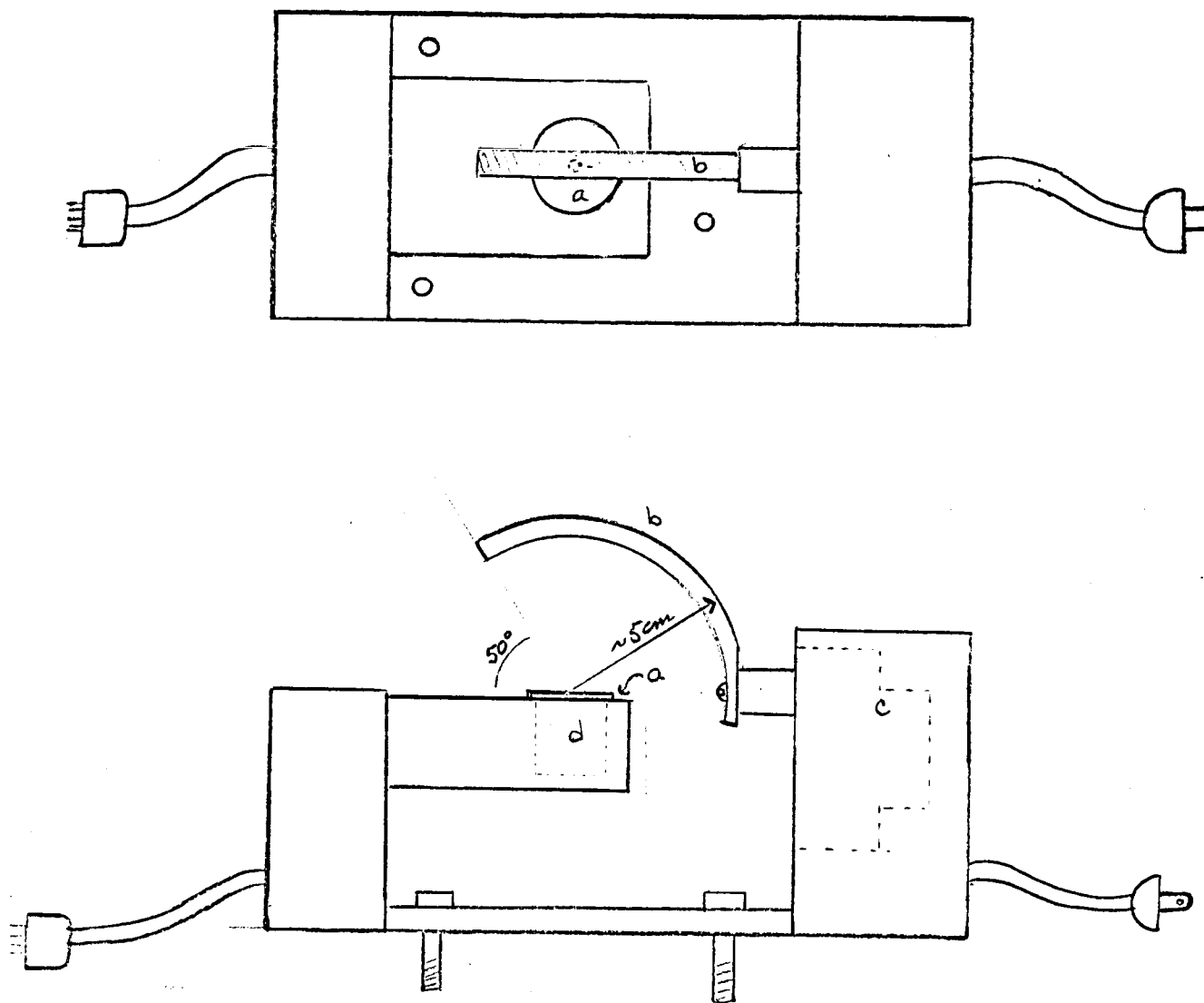


Figure 2 Sketch of the Moving Bar Occulting Radiometer (MBOR)

- a - Aperture plate
- b - Shade bar
- c - Motor housing
- d - Detector

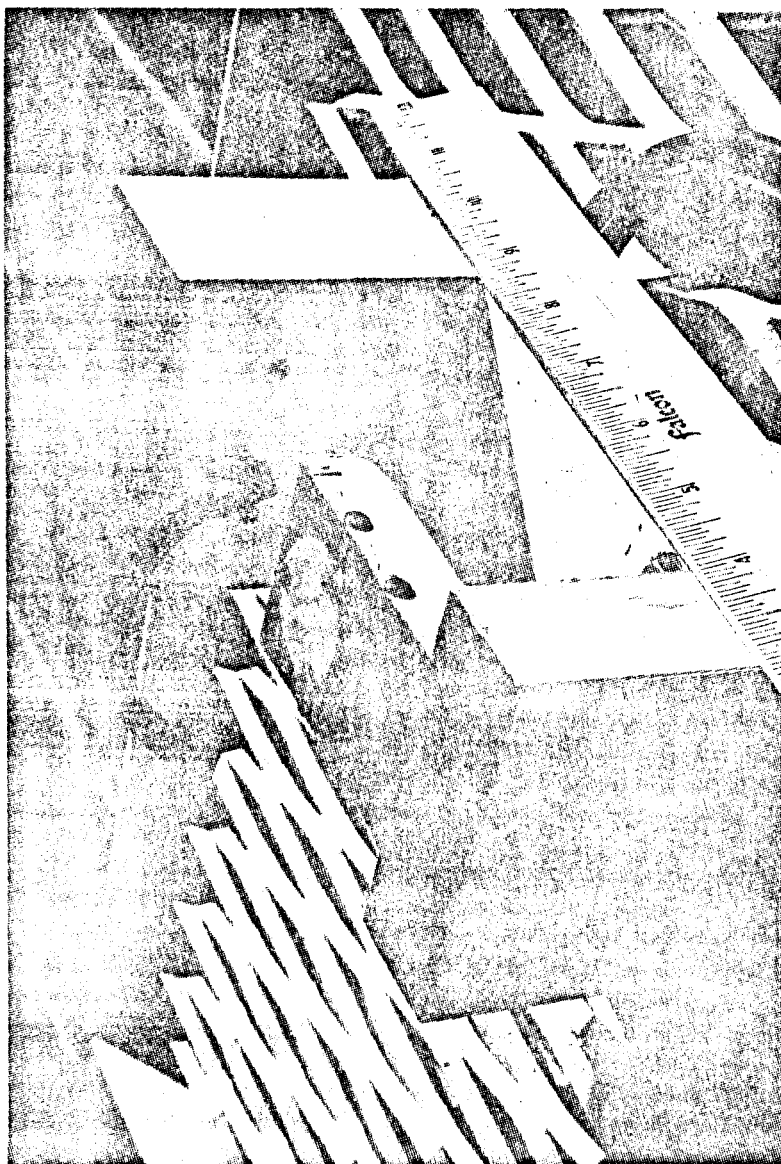


Figure 3 Photograph of the Moving Bar Occulting Radiometer (MBOR)

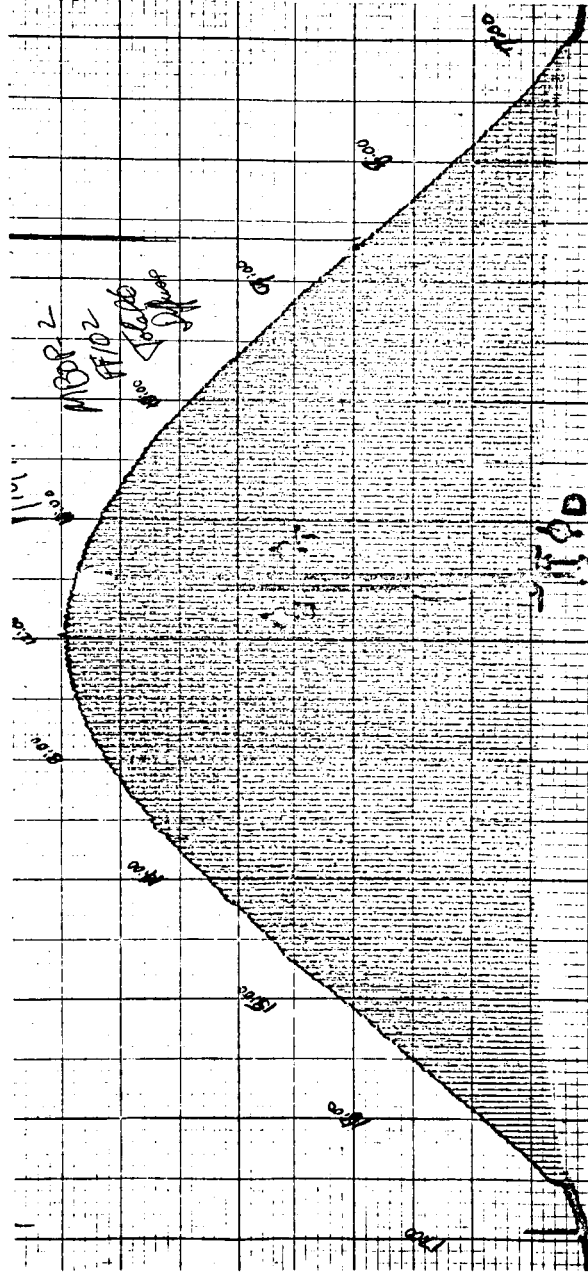


Figure 4 Typical clear-day output from the Moving Bar Occulting Radiometer (MBOR)

aperture plate as shown in detail in Fig. 5. The area immediately above the detector locating sleeve, and just under the aperture plate houses a neutral density filter required to keep some detectors from saturating at the maximum flux levels. One of the features of this simple instrument is that the form of the analog output renders a good visual representation of the relative amounts of the three flux quantities. However, a digital readout of the data from this instrument is difficult. It is advantageous to be able to process the data for calibration and statistical analysis. Computer compatible digital readouts would reduce the labor required for these analyses. The MBOR presents a problem regarding digital readout due to the difficulty in specifying the position of the occulting bar when measuring ϕ_D . There is no simple way to specify whether a change in the output is due to an occultation by the bar or by a cloud.

An alternate design which does facilitate a digital output format is the Fixed Bar Occulting Radiometer (FBOR). This instrument, shown in the sketch in Fig. 6, and in the photograph in Fig. 7, consists of a circular bar oriented East-West around the detector plane. The ring slides along an axis tilted with respect to the horizontal by an angle equal to the local latitude (32.2° for Tucson). The motion of the bar along this axis adjusts for the seasonal variation of the solar declination. The occulting bar has a diameter of 30.5 cm, and its width, from Eq. (1) is 5.6mm. The occulting bar is placed so that at the equinoxes its center of curvature will coincide with the center of the aperture over one of

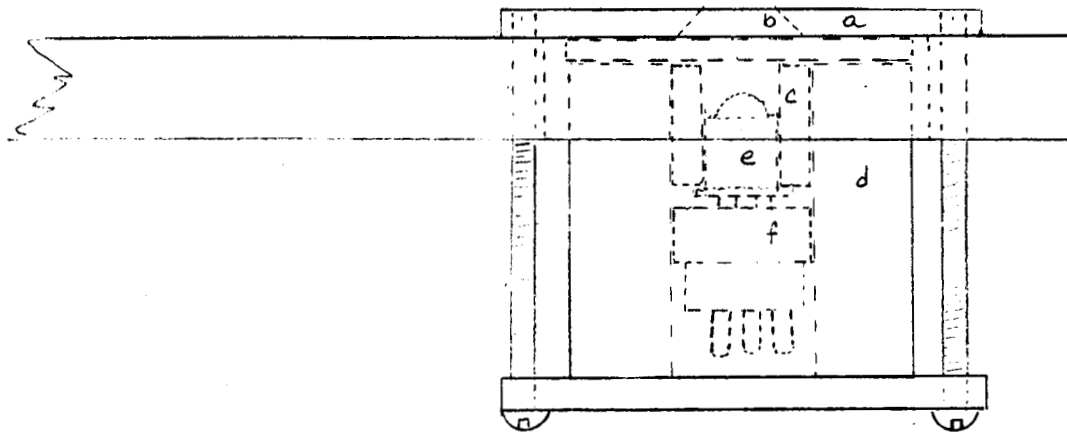


Figure 5 Detector cell design for the MBOR

- a - Aperture plate
- b - Diffuser
- c - Detector locating sleeve
- d - Cell cylinder
- e - Detector (T0-5 can)
- f - Transistor socket

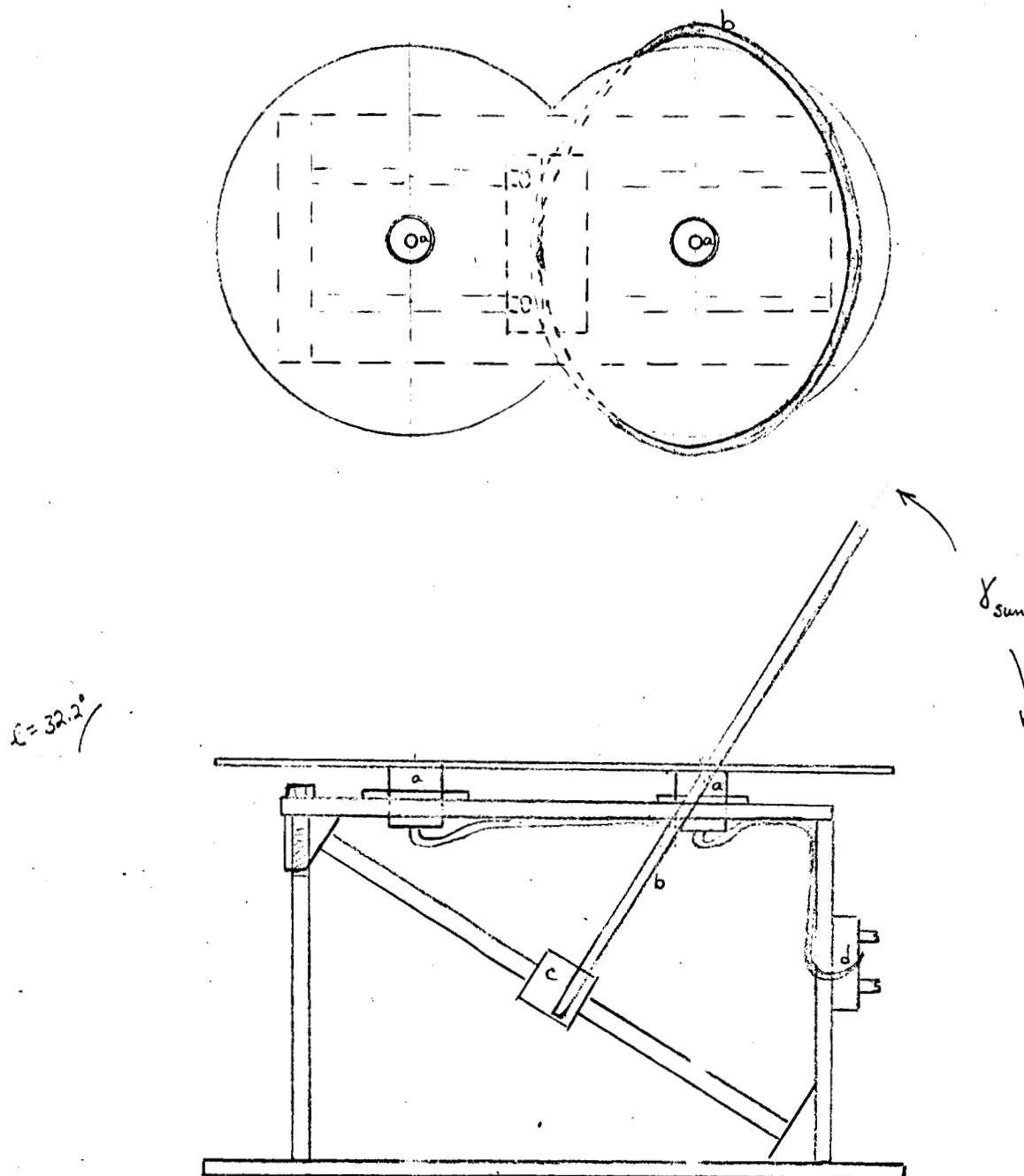


Figure 6 Sketch of the Fixed Bar Occulting Radiometer (FBOR)

- a - Detector cells
- b - Occulting bar
- c - Slider assembly
- d - Terminal block, electronic outputs

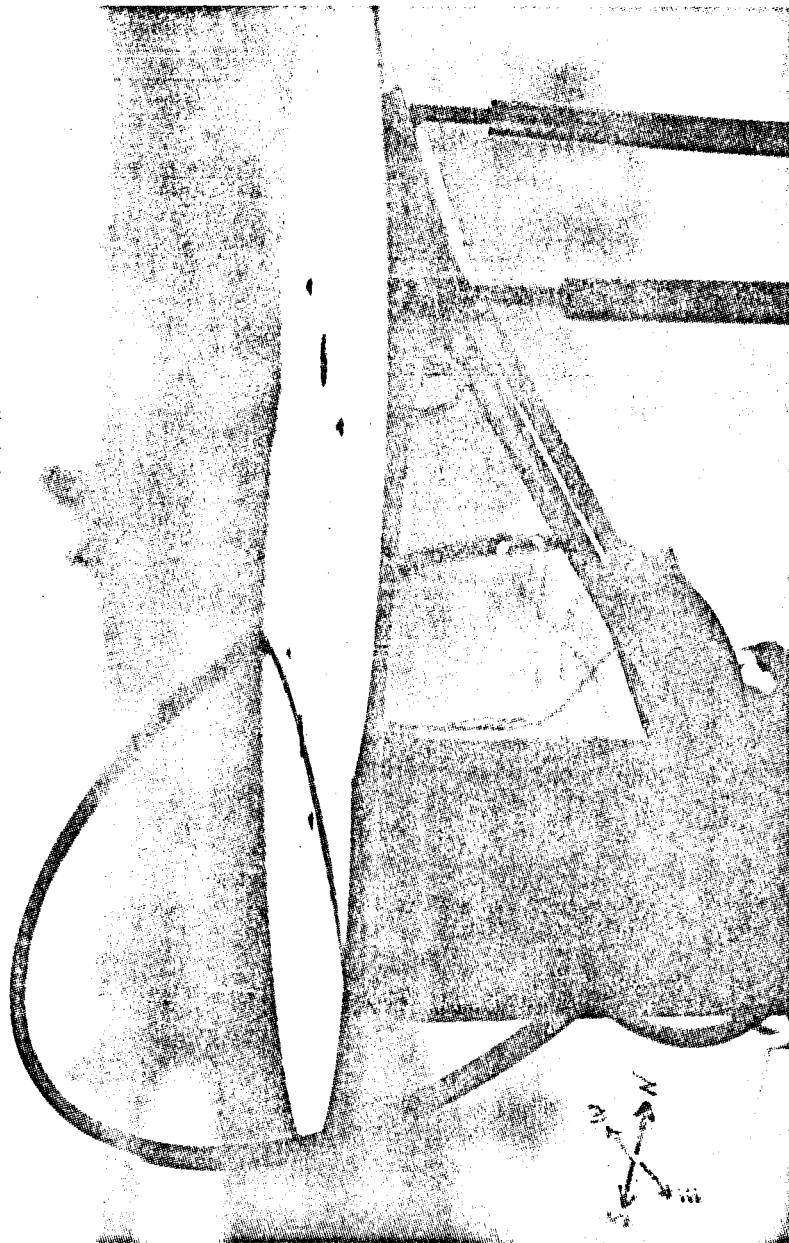


Figure 7 Photograph of the Fixed Bar Occulting Radiometer (FBOR)

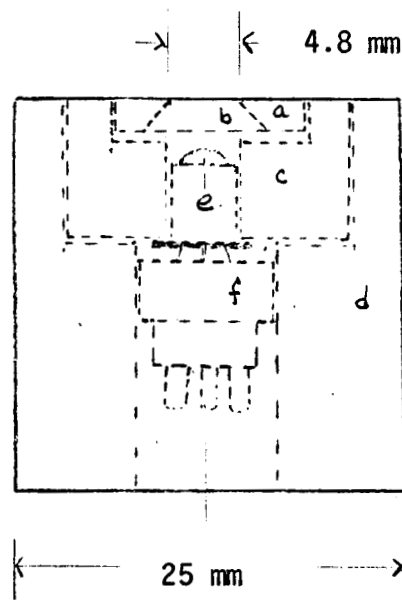


Figure 8 Detector cell design FBOR

- a - Aperture plate
- b - Diffuser
- c - Detector locating sleeve
- d - Cell cylinder
- e - Detector (T0-5 can)
- f - Transistor socket

the detectors. A second detector is mounted close to the first, but always out of the shadow. The first detector, therefore, measures only the diffuse or sky radiation while the second measures the total flux. The FBOR was the first of the instruments to be designed and built. The detector cells employed in this design were found, during the tests, to be inferior to the MBOR cell design. New cells have been designed and will be installed in the FBOR in the near future. An instrument tower was designed and constructed as shown in the photographs in Fig. 9. The 6-meter high instrument platform allows a nearly unobstructed view of the horizon for the instruments. Access to the instruments is by ladder to a lower landing, placed so that the equipment is at chest level. The tower has been found to be stable enough to insure accurate tracking for the pyrheliometer.

The accuracy of the measurements, the reliability, and complication of the instruments all depend on the choice of the detector. There is a wide choice of types of detectors suitable for radiometric use. In general, detectors fall into two categories that typify the mode of operation: 1) photoelectric devices such as photodiodes, photomultipliers, and photo-transistors, and 2) thermal divices such as thermal piles, pyroelectrics and thermistors.

The selection criteria for a detector should include the following:

- 1) quality and long service life
- 2) operating temperature range from -10 to $+70^{\circ}\text{C}$
- 3) high sensitivity over the range $0.3\mu\text{m} < \lambda < 1.5\mu\text{m}$
- 4) flat spectral response over the same range
- 5) suitability to radiometric use

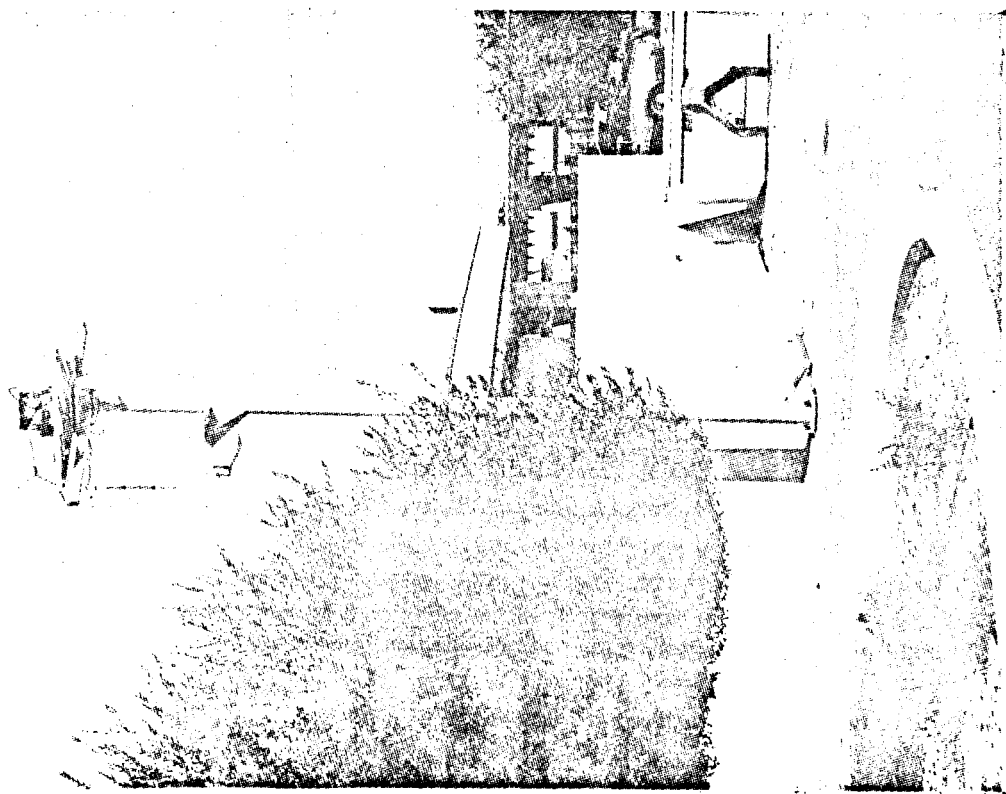
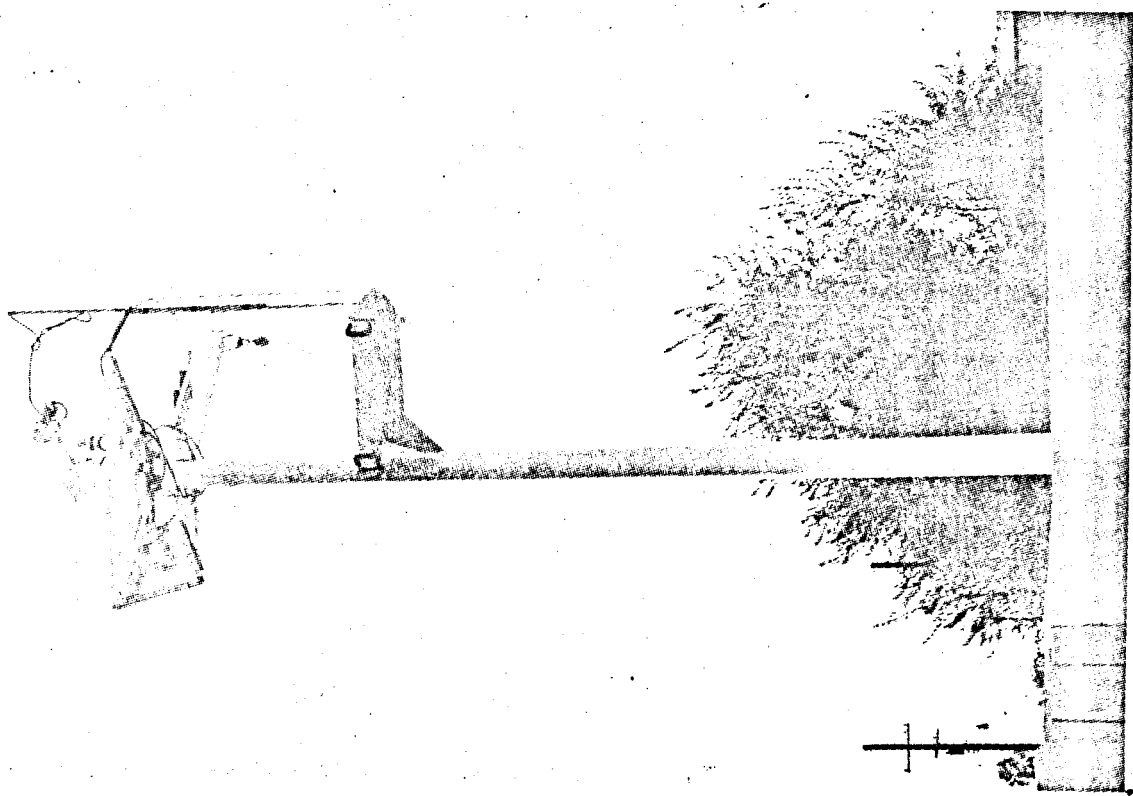


Figure 9 Photographs of instrument tower

6) reasonable cost

7) simplicity of use.

When available detectors are judged on the basis of these criteria, there are advantages and disadvantages for each detector type.

The best candidate for this application among the photoelectric devices is either a photodiode or a phototransistor. The photodiodes have two modes of operation. In the photovoltaic mode, the diodes generate outputs that are either linear or logarithmic depending on the load resistance. The photodiodes have a distinct advantage with nearly zero null drift in the photovoltaic mode. Photodiodes can also be used as photoconductors but show temperature drift when used in this manner. The sensitivity of photodiode - operational amplifier combinations described below is well matched to solar measurement applications. Photodiodes come in small, simple packages such as TO-5 transistor cans. One disadvantage for photodiodes is the characteristic spectral response for the silicon device. The peak sensitivity is usually in the near infrared between $0.8\mu\text{m}$ and $0.9\mu\text{m}$ with lower response in the near ultraviolet. It is not difficult to use such a device, and compensate for the spectral response by calibration or filtering.

Photo transistors are limited to the photoconductive mode with the inherent zero drift problems. Photo transistors with base connections can also be used as photodiodes. The availability of other positive factors could render this class of device useful for this application.

The thermal devices have an advantage in their flat spectral response over wide spectral ranges. The response of these devices depends only on the type of absorber coating used to convert the incident radiation into heat. Since good absorbing surfaces are available for the ultraviolet through the far infrared, thermal devices are usable at almost all wavelengths. Thermistors are among the more expensive devices considered. They are also limited in their operating temperature range and often require cooling. Pyroelectrics, on the other hand, can operate at temperatures up to the curie point of the pyroelectric material which is usually about 50-70°C. These detectors also have a flat spectral response, but require a chopped input light signal for proper operation. Of the thermal detectors, the simplest is the thermal pile. This detector can operate without chopping and at temperatures up to 125°C, and is frequently used for solar measurements. The use of such a detector, however, requires care in excluding unwanted infrared radiation from the detector. The flat spectral response is a desirable characteristic.

Silicon photodiodes were selected for this application because of their numerous advantages. The lack of a flat spectral response is easily correctable and not judged to be a serious disadvantage. The United Detector Technology 3DP pin photodiode was selected as the primary detector after comparative testing of other similar detectors. Silicon photodiodes of this type have become more widely used with the development of improved output

electronics. Recent articles^{2,3,4} discuss the equivalence of silicon photodiodes, combined with an operational amplifier (op-amp) output circuit, to photomultipliers. This diode / op-amp combination gives a linear output and high sensitivity without the need for high voltages or a bulky detector. The principle reason for the op-amp is shown by the characteristic load curves for the diode shown in Fig. 10. From the graph one can see that at zero bias (photo-voltaic) and zero load resistance, one can get a linear response characteristic. The use of the op-amp as shown in Fig. 11 yields such a zero load condition and still maintains a large output signal. This is because the load on the photodiode is equal to the feed-back resistance R divided by the open loop amplifier gain G .

The actual circuit used in our case is shown in Fig. 12. Since the open loop gain of the LM741 is about 2×10^5 and the feed back resistance is about $2 \times 10^6 \Omega$, the photodiode sees a load resistance of about 10Ω . Figure 13² shows the deviation from linearity that can be expected for a cell that has an effective load resistance of this value. From the plot, one can see that even at currents as high as 1 mA, the device is linear to two parts in 10^5 (0.002%). One can calculate the actual current from the photodiode according to:

$$V_{\text{out}} = -R_f i_o$$

or

$$i_o = -V_f / R_f .$$

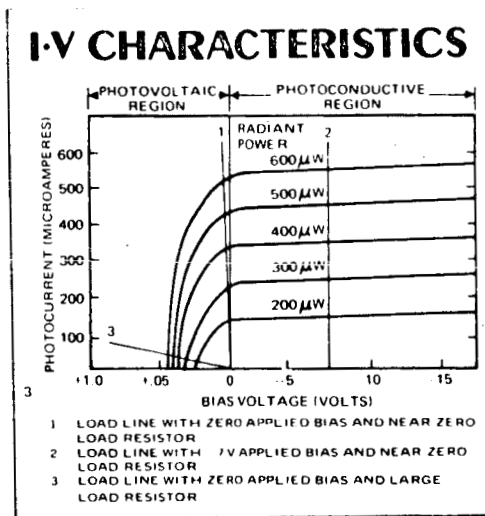


Figure 10 Load line plot for a typical photodiode (UDT3DP)

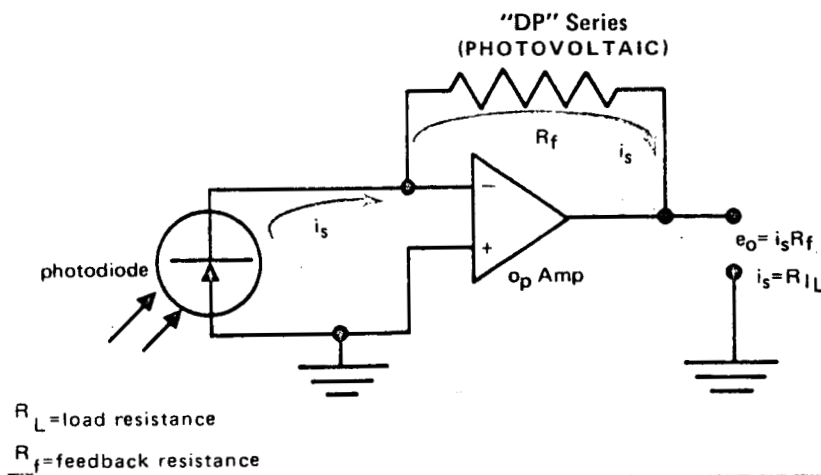
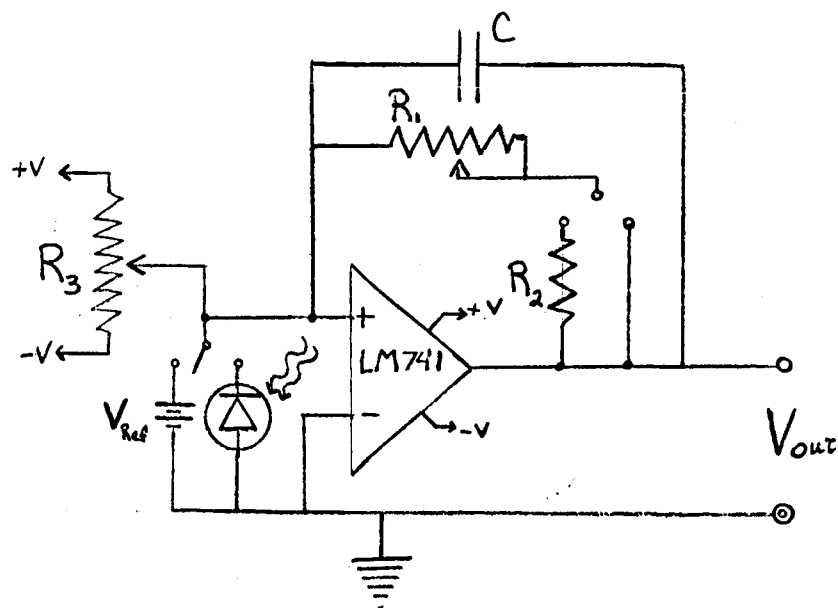


Figure 11 Circuit schematic for the photodiode - operational amplifier circuit. i_s = photodiode sensitivity x light flux, $R_L = R_f / G$ where G = open loop gain.



$$C = 0.047 \mu f$$

$$R_2 = 2 M\Omega$$

$$R_1 = 2 M\Omega$$

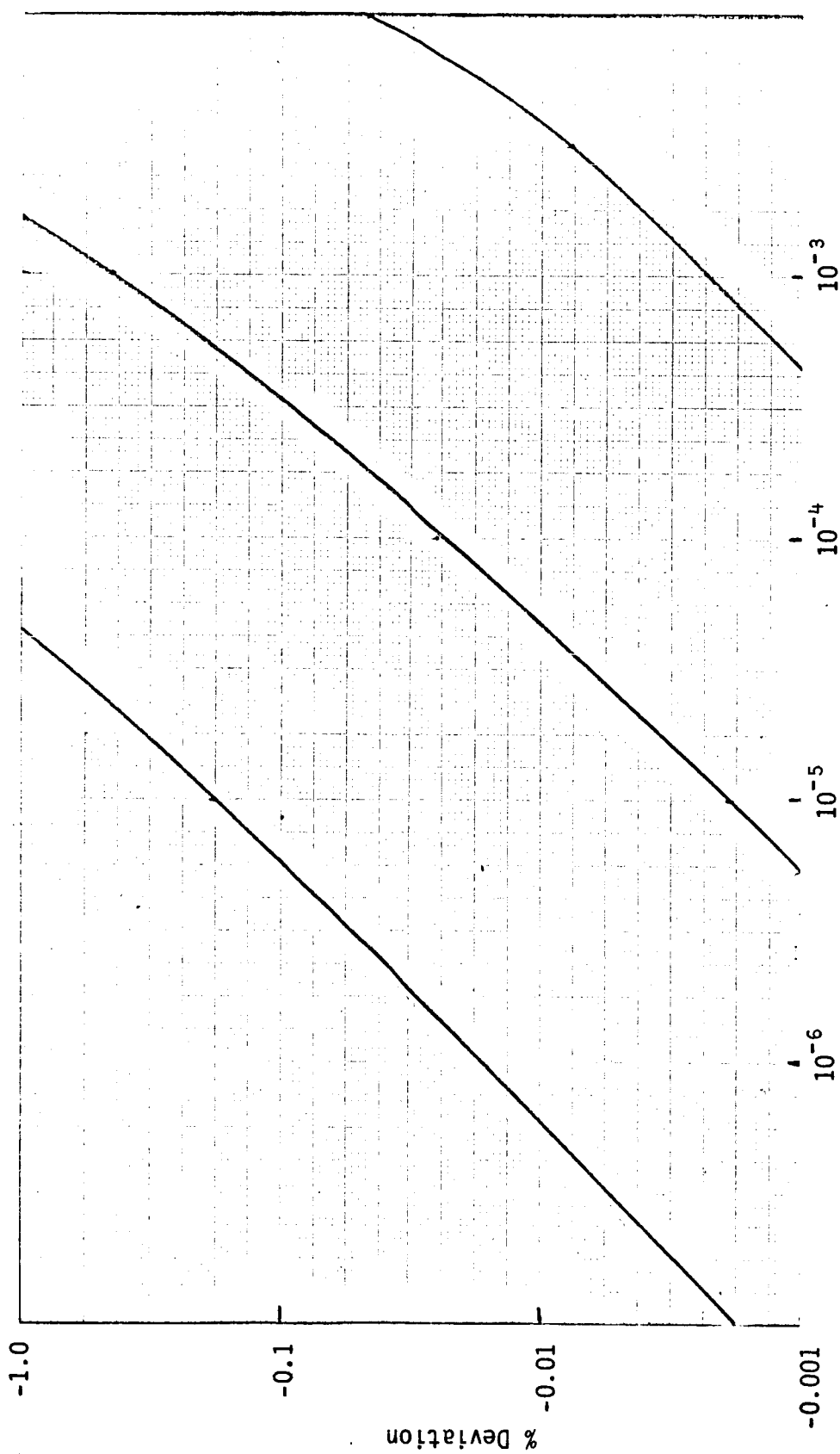
$$R_3 = 12 M\Omega$$

Figure 12 Schematic diagram of Helio circuit used for the current-to-voltage transducer.

R_1 , R_2 Feedback resistors ($R_f = R_1 + R_2$ or R_1)

R_3 Zero offset adjustment

V_{Ref} Reference voltage for circuit gain calibration



Cell Current I_C , Amperes

Figure 13 Deviation from linearity of the silicon cell response for short-circuit operation.

In our case, for the maximum flux level, $V_{out} \approx 0.8V$ for $R_f \approx 1.6 M\Omega$, so that $i_o \approx 2 \times 10^{-5}A$. Referring again to Fig. 13, we can see that the device is still within the linear region of operation for a 10Ω load.

After initial breadboarding and debugging, the op-amp circuits were checked for drift and noise pickup problems. The measured zero drift was less than 10 mV for a 1 V full-scale output level. Drift in the full scale settings due to gain drift was also less than 10 mV on the 1V full-scale level. In the initial breadboard layouts, another problem encountered was that more adjustment was required for the output offset than obtainable from the internal null adjustment on the LM741 op-amps. The use of these internal null circuits can also increase the amount of offset drift encountered. It was therefore decided to use the nulling scheme shown by R_3 in Fig. 12. Adjustment of R_3 allows the application of a balance voltage to the input to counteract the output offsets. The voltage drift with this type of null adjustment is smaller than with the internal null adjustments. We have not, as yet, confirmed this. In the near future, the circuits will be hard-wired on printed circuit cards, one card per detector, and will be mounted in a card bin for easy access. A means will be provided whereby a reference voltage or open circuit may be applied to the electronics for calibration of the gain setting, and input zero offset adjustment. It has been our experience to date, that zero light level and zero input voltage are equivalent. To insure this condition, however, and to calibrate

the whole system, the zero and gain adjustments will be checked periodically by covering the detector and by exposure of the detector to a one solar constant flux level from a standard source.

Task 2.3 Test

The two instruments MBOR and FBOR have been installed on the instrument platform for a period of two weeks. No operational problems remain unsolved. The instruments are ready for calibration on schedule.

Task 4 Data Analysis

The data analysis task has been somewhat delayed by difficulties encountered in the instrument development task that drew off more of the available manpower than originally anticipated. The definition of analysis requirements (Task 4.1) is in progress at this time.

During the past two weeks, some preliminary data were gathered for comparison with the standard National Weather Service Data and to check out the operations and adjustments. Although our data have not been fully calibrated, we can examine two points of interest:

1. Whether the frequencies of cloud occultation are similar for the two sets of data
2. Whether the instruments are in agreement as to the solar flux readings at any hour angle.

The University and Helio installations are separated by a distance of 16Km on a relatively flat triangular shaped valley floor which is rimmed on all three sides by mountains. The separation and relative proximities to the mountains could cause considerable differences in the readings at any time on partly cloudy days. However, the examples of instrument outputs shown in Figure 14 and 15 indicate good agreement as to the shape of the data curves for the two stations. The data shown in Figure 14a and 15a are from the MBOR. The data in Figure 14b and 15b are from the University of Arizona Eppley pyranometer. A close look at Figure 15 shows good correlation for the cloud activities around 9:00, 12:00, and 15:00 hours. The increases in the flux due to reflections from the clouds are also in agreement. These reflections result in the "bumps" in the curves at ~9:00 and 15:30 on both plots.

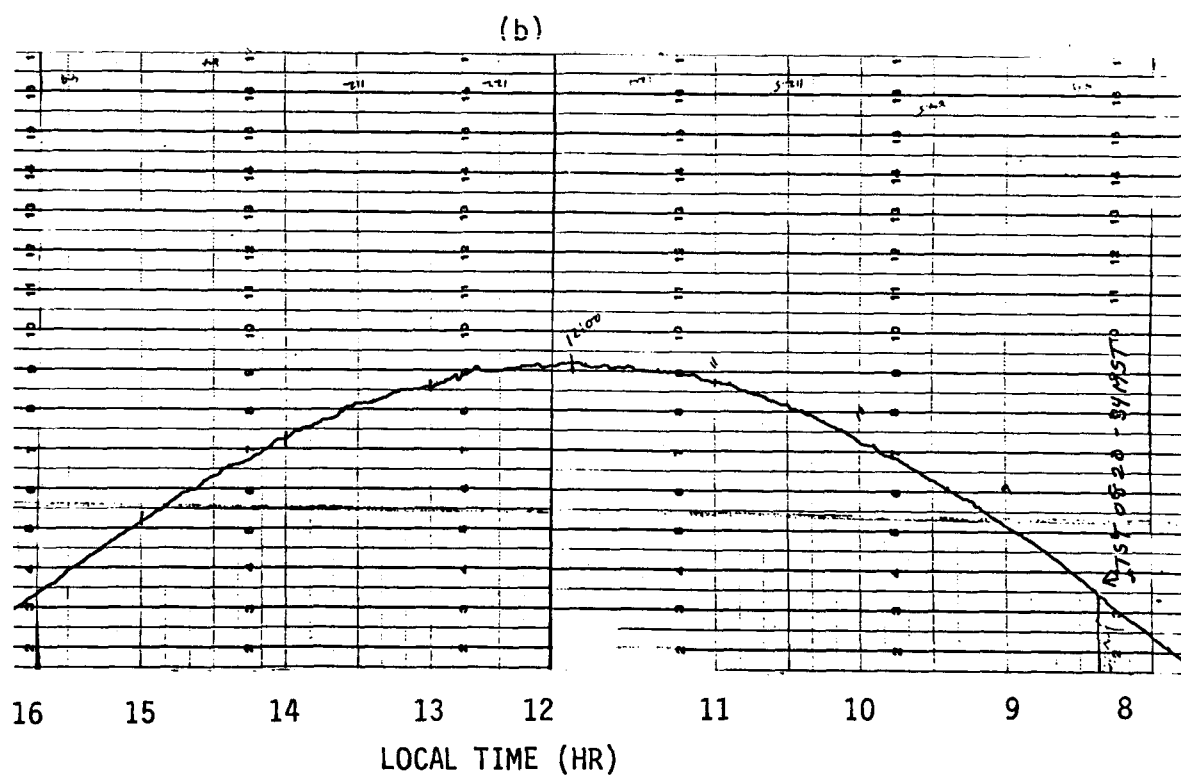
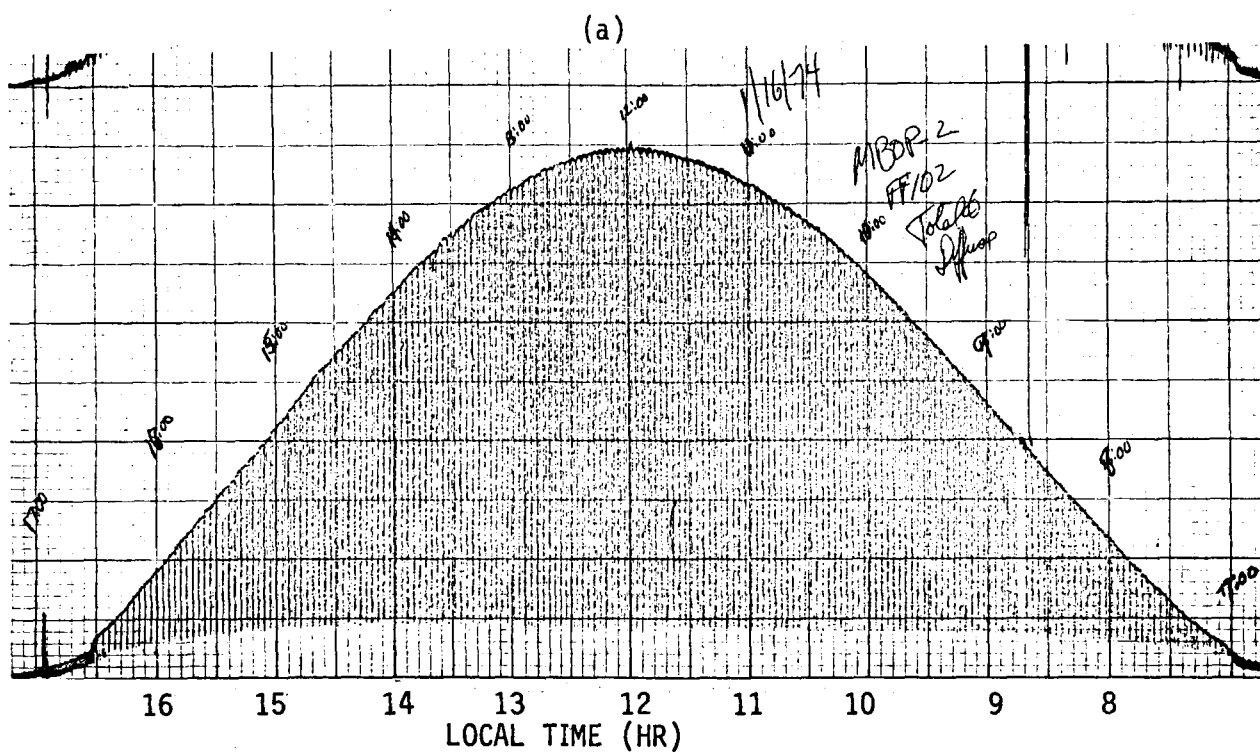


Figure 14 Recorder output 1/16/74 showing clear day comparison between (a) MBOR and (b) U/A records.

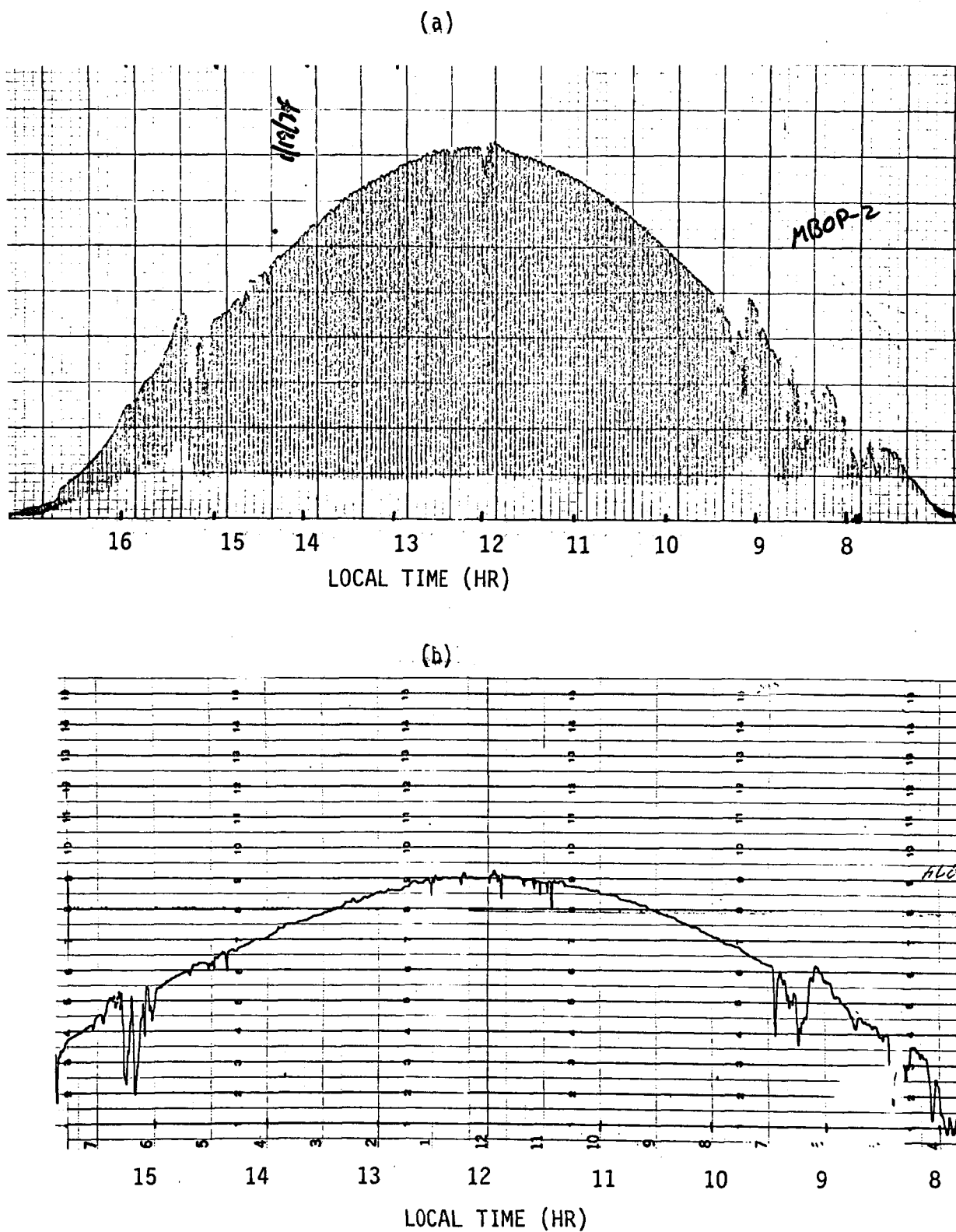


Figure 15 Recorder output 1/19/74 showing partly cloudy day comparison between (a) MBOR and (b) U/A records

This suggests that although there are minor differences due to cloud structures, the overall occultation pattern is the same. The records included in Figures 14-17 are also representative of the general types of days observable. Based on the current data, and about 6 months observations done with an earlier prototype, we can class the types of MBOR records, according to their general shape, into three groups. The most predominate type of day is the clear or almost clear day. The record of this type of day shows a regular pattern like that shown in Figures 14 and 15. The second type of day is characterized by rapid variations in the flux, with periods less than 15 minutes. The record shown in Figure 16 is characteristic for such days and is typical for high thin clouds. A heavy overcast sky is the third type of day. On such days, the record looks like that shown in Figure 17, where the direct flux is low most of the time. The data shown in Figures 16 and 17 are also from the MBOR as installed at the Helio site. As one part of the data analysis for this project, we expect to be able to describe, in detail, the frequency of occurrence for each type of day. In addition, we will look in some detail at the lengths of occultation within these active days, and the resulting flux levels. At this point in the program, we can compare the data gathered at the University and Helio, examining the point by point similarity of the two records. This can obviously be done only on clear days. The measured values of the flux at any one time should be nearly identical because the only atmospheric effects on ϕ are due to slight differences in the local turbidity of haze levels.

The measured data for the total insolation are given in Table 1 for the MBOR and the Eppley pyranometer from the University of Arizona for

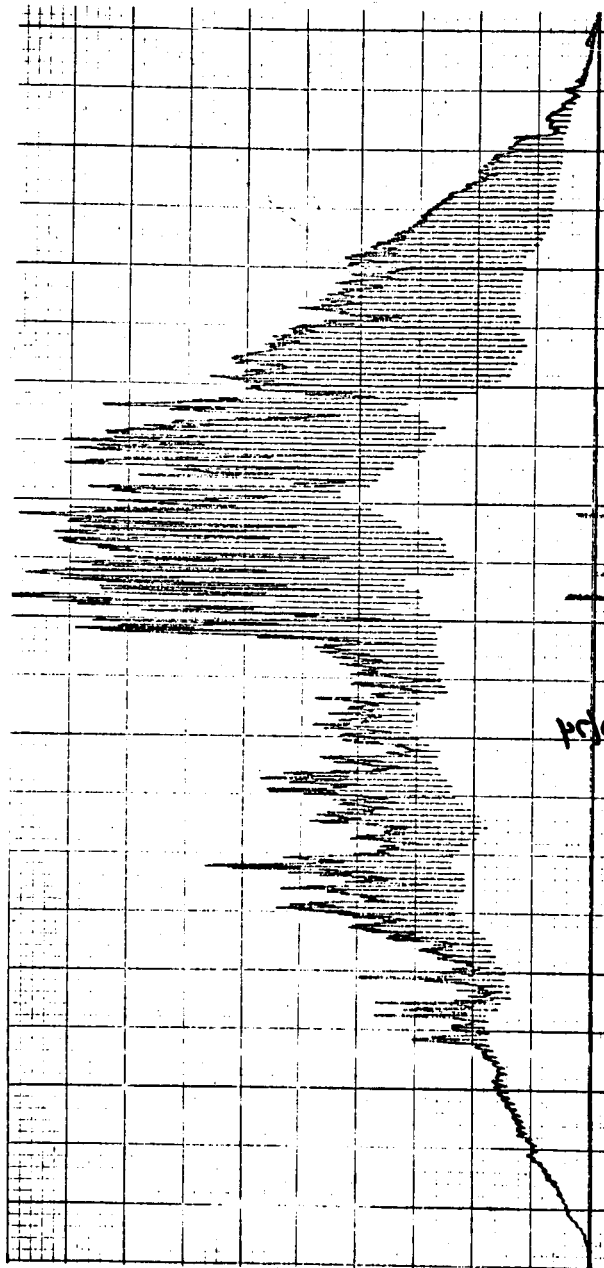


Figure 16 MBOR recorder output showing pattern typical for day
with high thin clouds.

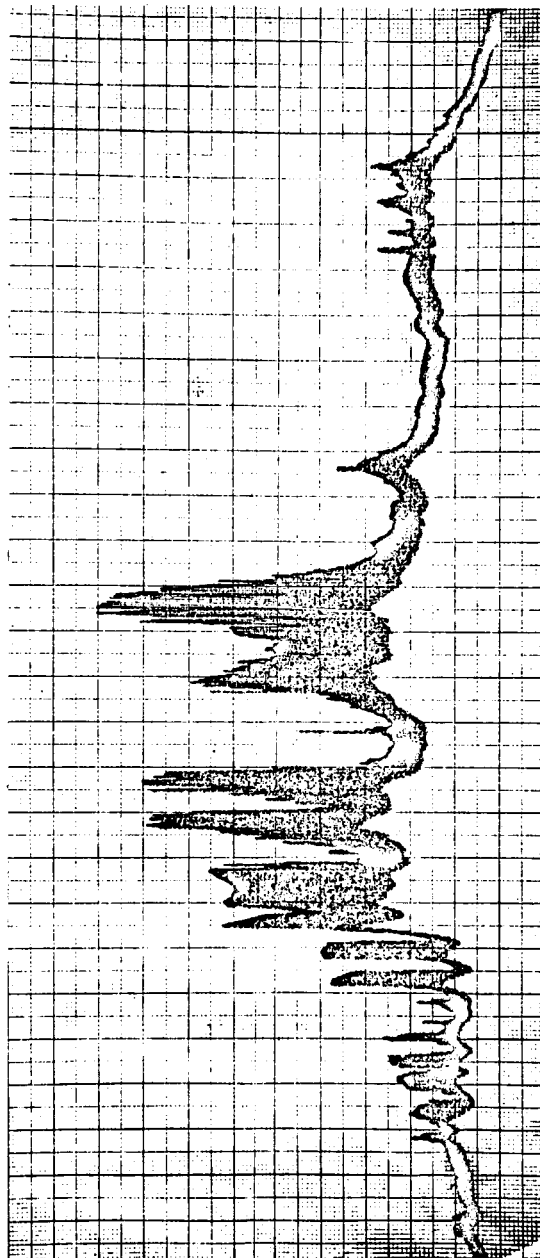


Figure 17 MBOR recorder output showing pattern typical for an overcast day.

Date	Local Time (hours)	ϕ * MBOR	ϕ * U/A	$R_m = \frac{\phi \text{ MBOR}}{\phi \text{ U/A}}$
1-16-74	8	.253	.282	.897
	9	.545	.515	1.058
	10	.787	.725	1.085
	11	.962	.872	1.103
	12	.968	.925	1.046
	13	.901	.860	1.047
	14	.735	.725	1.014
	15	.518	.515	1.006
	16	.269	.335	.802
1-18-74	8	.193	.225	.858
	9	.492	.487	1.010
	10	.652	.685	.952
	11	.837	.860	.973
	12	.885	.910	.972
	13	.820	.850	.964
	14	.742	.755	.982
	15	.500	.545	.917
	16	.209	.195	1.07
1-19-74	8	.236	.190	1.242
	9	.533	.572	.932
	10	.687	.715	.961
	11	.868	.850	1.021
	12	.881	.900	.978
	13	.842	.855	.984
	14	.706	.705	1.001
	15	.537	.500	1.07
	16	.329	.295	1.115
Average				1.002 \pm 5.7%

*Flux Units - Langleys/minutes

TABLE 1 COMPARISON OF TOTAL FLUX MEASUREMENTS

three relatively clear days. As one can easily see, the agreement is not exact. This is due partially to the fact that only a preliminary calibration exists for the MBOR and to the 16Km separation between the instruments. We also calculate the ratio of the two measurements R_m where $R_m = 1.0$ would indicate exact agreement $R_m > 1.0$ shows that our readings are larger than those at the University. Since our sensor is farther from the metropolitan center, we would expect $R_m > 1$. The more significant factor is that the average value of R_m is 1.002 with a probable error of $\pm 5.7\%$. This level of disagreement is within our expectations at this time, and we expect to be able to show significant improvement after completion of the detailed calibration in Task 3.

III. CURRENT PROBLEMS

The only problem encountered to date has been the unexpectedly long delivery time for the Eppley pyrhelimeter. Other items are also being delayed, but no extraordinary delays in the original program schedule are anticipated at this time.

IV. WORK PLANNED FOR NEXT PERIOD

The final steps preparatory to daily observations will be completed in the next period. These include final wiring of amplifier circuits, installation of the digital recorder, and full calibration of the instruments. In addition, programming for the data analysis task will be initiated. If no problems are encountered, we would anticipate having an automatic data reduction capability by the end of the next two months.

REFERENCES

- 1 *Solar Radiation*, N. Robinson (Ed.), Elsevier Publishing Co., New York 1966.
- 2 P.G. Witherrell & M.E. Faulhaber, *Applied Optics*, 9, 73, (1970).
- 3 R.H. Hamstradt, Jr. & P. Wendland, *Applied Optics*, 11, 1539, (1972).
- 4 G. Ruffino, *Applied Optics*, 10, 1241, (1971).